

The Path From the Simple Pendulum to Chaos

Josh Bevino

Department of Physics
Colorado State University

lxmn1234@rams.colostate.edu

Report submitted to Prof. P. Shipman for Math 540, Fall 2009

Abstract. This paper fully discuss the dynamics of the damped driven pendulum. The governing equations of the dynamics are derived. The linear dynamics of the pendulum are discuss in the cases of small angles approxiamions and no driving forces. The non-linear dynamics when the driving force is involved are discussed. Many mathematical tools are used for analysis

Keywords: Driven Damped Pendulum, Chaos, Poincaré Section,

1 Introduction

The pendulum is a very interesting dynamical system to study. In early studies, young students use approximations to find the equation of motion of the pendulum. Next, students are exposed to numerical methods for solving the more complicated pendula systems. This paper's goal is to focus on analytical methods for solving the equation governing the pendulum's motion. Often there will not be a solution; however, there will be tools that yield information about equation for motion and give the student the ability to confidently discuss the motion of the pendulum.

This paper is organized as follows: In Section 2, we discuss the physical pendulum, and derive the governing equation of motion. In Section 3, we discuss the simplest model of the pendulum with neither damping nor driving forces. In Section 4, we discuss, the next step in difficulty, of a model of the pendulum which includes the damping force. In Section 5, we discuss the damped driven pendulum and find chaos, both in numerical sumulations of a dynamical system and in a experimental system, the EM-50 Chaotic Pendulum constructed by the Daedalon Corporation. In section 6, we summarize the findings of this paper.

2 The Physical Pendulum

Let us begin with the rotational analog to Newton's equation:

$$\sum \Gamma = I\alpha \tag{1}$$

Define the following:

Torque as Γ

The direction of positive toque as out of the page

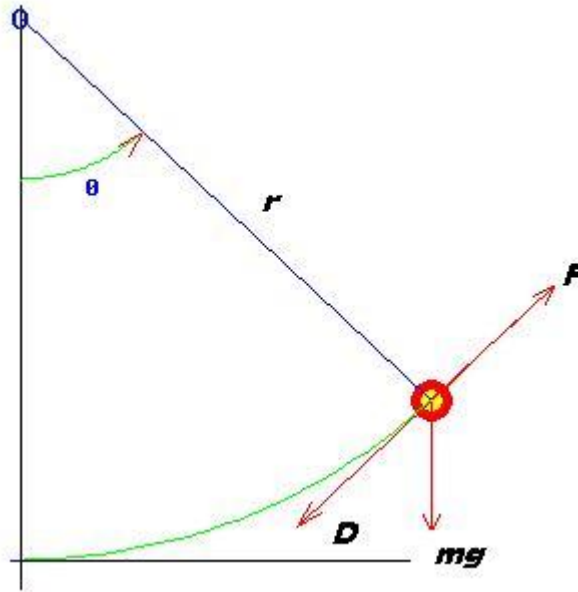


Figure 1: Schematic of a pendulum

I as the moment of inertia equal to mr^2 , the theoretical pendulum is modeled as a point mass. Angular Acceleration as α , also $\ddot{\theta}$, which is the second derivative w.r.t. time of Angular Position θ
 $v = r\omega = r\dot{\theta}$

Using fig. (1) one can begin deriving the equation of motion for the pendulum. Equation (1) becomes, by use of $\vec{\Gamma} = \vec{r} \times \vec{F}$:

$$-damping_{force} - gravity_{force} + driving_{force} = I\ddot{\theta} \quad (2)$$

$$-bvr \sin \theta + -mgr \sin \theta + Fr \sin \theta = I\ddot{\theta} \quad (3)$$

Let the damping and driving forces be parallel to the motion of the pendulum. Let the driving force be a function of time. Let $D = bv$, so the damping force is dependent on velocity, v or $r\dot{\theta}$. Rearranging and substituting:

$$mr^2\ddot{\theta} + br^2\dot{\theta} + mgr \sin \theta = F(t)r, \quad (4)$$

$$\ddot{\theta} + \frac{b}{m}\dot{\theta} + \frac{g}{r} \sin \theta = \frac{F(t)}{mr}. \quad (5)$$

Equation (5) is the second order differential equation describing the dynamical system of interest.

3 Simple Pendulum

The simplest dynamics occur by letting $F(t) = 0$, $b = 0$, and by use of the small angle approximation $\sin \theta \approx \theta$. However, this yields the extremely well-known solution of simple harmonic motion. We will not analyze this case. Let us just forget about the small angle approximation letting $F(t) = 0$ and $b = 0$ still. Equation (5) now becomes:

$$\ddot{\theta} + \frac{g}{r} \sin \theta = 0. \quad (6)$$

Let us nondimensionalize the system, following Strogatz [1]:

Two variables have units in eq. (6) dt and $\frac{g}{r}$. Imagine attempting to get a $\frac{g}{r}$ term along with $\ddot{\theta}$, so you could multiply eq. (6) by $\frac{r}{g}$ and remove the units. So we want dt^2 to be equal to a variable that when we write $d^2\theta$ divided by that variable the $\frac{g}{r}$ term appears. Let us write eq. (6) differently.

$$\frac{d^2\theta}{dt^2} + \frac{g}{r} \sin \theta = 0 \quad (7)$$

Now the variable discussed in the previous paragraph is:

$$dt^2 = \frac{r}{g} d\tau^2. \quad (8)$$

Substitute (8) into (7);

$$\frac{g}{r} \frac{d^2\theta}{d\tau^2} + \frac{g}{r} \sin \theta = 0 \quad (9)$$

$$\ddot{\theta} + \sin \theta = 0 \quad (10)$$

Note eq. (10) is written in standard dot notation; however, the derivative is to be taken with respect to the dimensionless time variable τ .

Now we will begin working with eq. (10). Eq. (10) is a 2^{nd} order differential equation which we can write as two 1^{st} order differential equations, to begin working with the linearized system. We will compute the Jacobian Matrix at fixed points.

Defining $\dot{\theta} = y$, eq. (10) becomes

$$\dot{\theta} = y = f(\theta, y), \quad (11)$$

$$\dot{y} = -\sin \theta = g(\theta, y). \quad (12)$$

The Jacobian is

$$\begin{pmatrix} \frac{\partial f}{\partial \theta} & \frac{\partial f}{\partial y} \\ \frac{\partial g}{\partial \theta} & \frac{\partial g}{\partial y} \end{pmatrix}_{(\theta^*, y^*)} = \begin{pmatrix} 0 & 1 \\ -\cos \theta & 0 \end{pmatrix}_{(\theta^*, y^*)}.$$

The fixed points can be directly discovered from eqs. (11) and (12). They occur when the right-hand sides are equal to zero, meaning there is no change in θ or y . The fixed points occur when $(\theta, y) = (n\pi, 0)$. Evaluated at the fixed points, the Jacobian becomes

$$\begin{pmatrix} 0 & 1 \\ \pm 1 & 0 \end{pmatrix}. \quad (14)$$

From the Jacobian we can use the characteristic equation to find the eigenvalues.

$$\lambda^2 - (\pm 1) = 0 \quad (15)$$

$$\lambda^2 - 1 = 0 \Rightarrow \lambda^2 = 1 \Rightarrow \lambda = \pm 1 \quad (16)$$

$$\lambda^2 + 1 = 0 \Rightarrow \lambda^2 = -1 \Rightarrow \lambda = \pm i \tag{17}$$

From this we discover hyperbolic equilibrium points when $(\theta, y) = ((2n + 1)\pi, 0)$ and non-hyperbolic equilibrium points when $(\theta, y) = (2n\pi, 0)$. The Hartman-Grobman states that for hyperbolic equilibrium points the linearized flow is topologically conjugate to the non-linearized flow in some neighborhood of the fixed point.

Although the Hartman-Grobman theorem does not give us information about the non-hyperbolic fixed points for the linearizations, we may use phase plane analysis to analyze the system at the non-hyperbolic fixed points. The vector field and some trajectories are plotted in fig. (2) using pplane7.m in MATLAB. This phase plane plot demonstrates that the fixed points are centers. This happens to be consistent with the linear analysis. Earlier, it was stated that the approximation $\sin \theta = \theta$ would not be made. However, in fig. (2), one can see the centers represent the case of the simple harmonic oscillator with the small angle approximation revealing the solution to the simplest case. The linearization near the fixed points is shown in fig. (3), also generated by MATLAB.

The Poincare-Bendixson theorem implies chaos is not possible in the two dimensional phase plane. The dynamical system, Eq. (10) is confined to the phase plane; therefore, chaos is not possible.

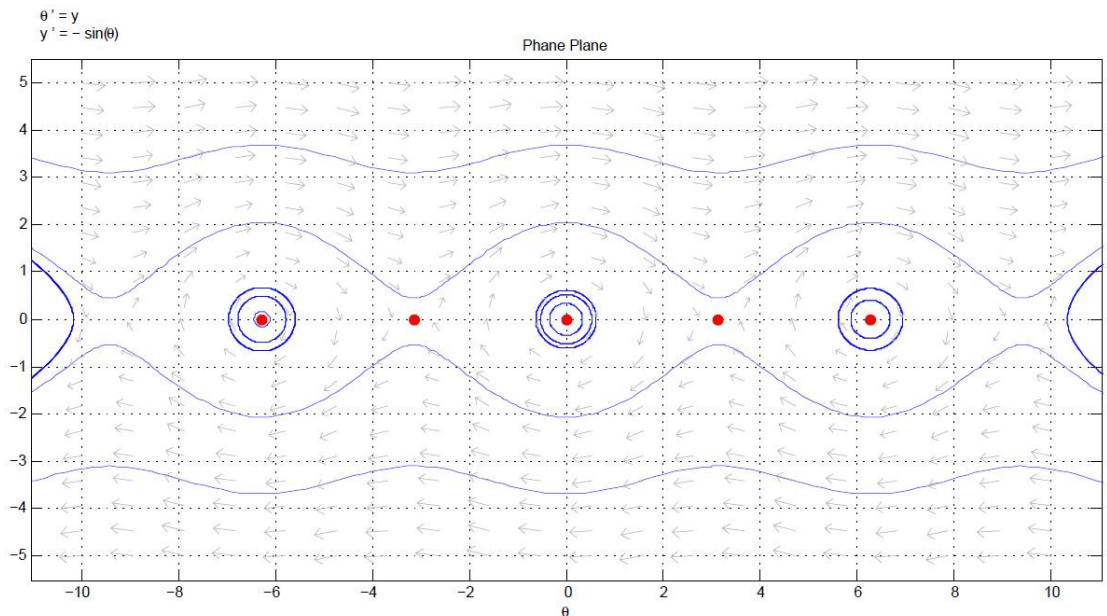


Figure 2: Phase plane of the simple pendulum

4 Will Damping Lead to Chaos?

Setting $F(t) = 0$, in eq. (5), we are left with

$$\ddot{\theta} + \frac{b}{m}\dot{\theta} + \frac{g}{r}\sin \theta = 0. \tag{18}$$

Again we will reduce the number of parameters:

$$dt^2 = \frac{r}{g}d\tau^2 \tag{19}$$

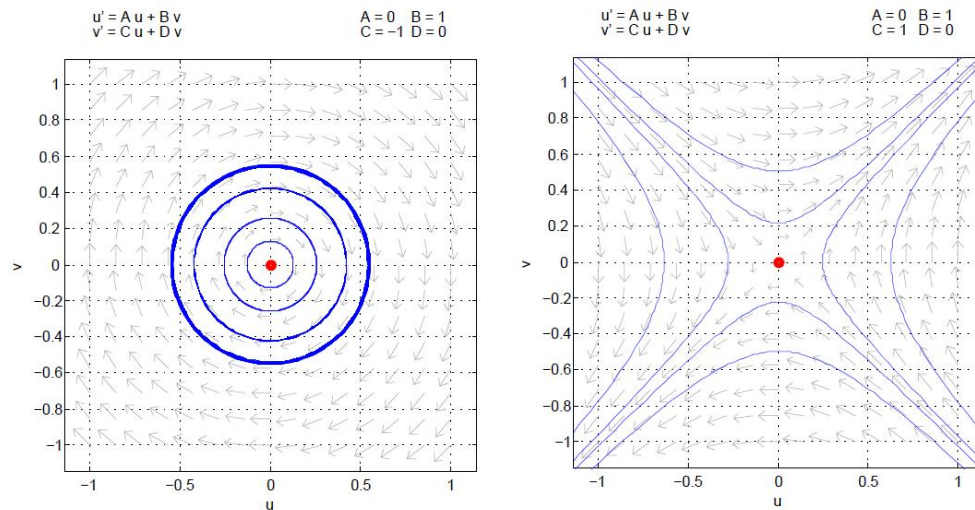


Figure 3: *Left:* The linearization about the fixed points $(\theta, y) = (2n\pi, 0)$ and *Right:* the fixed points $(\theta, y) = ((2n + 1)\pi, 0)$.

Substituting eq. (19) into eq. (18), and letting, $\beta = \sqrt{\frac{g}{r} \frac{b}{m}}$, we obtain after simplification the equation,

$$\ddot{\theta} + \beta \dot{\theta} + \sin \theta = 0. \tag{20}$$

Again, we will begin working with the linearization of eq. (20). Defining $y = \dot{\theta}$, eq. (20) yields

$$\dot{\theta} = y \tag{21}$$

$$\dot{y} = -\beta y - \sin \theta \tag{22}$$

The Jacobian of this system is

$$\begin{pmatrix} 0 & 1 \\ -\cos \theta & -\beta \end{pmatrix}_{(\theta^*, y^*)}. \tag{23}$$

The fixed points of eqs. (21) and (22) are $(\theta^*, y^*) = (n\pi, 0)$. The Jacobian evaluated at the fixed points becomes

$$\begin{pmatrix} 0 & 1 \\ \pm 1 & -\beta \end{pmatrix}. \tag{24}$$

The characteristic equation is now also affected by the parameter β . Next, consider the specific case for fixed points when $(\theta^*, y^*) = (2n\pi, 0)$. The Jacobian is

$$\begin{pmatrix} 0 & 1 \\ -1 & -\beta \end{pmatrix}, \tag{25}$$

and the characteristic equation is

$$-\lambda(-\beta - \lambda) + 1 = 0. \tag{26}$$

Solving for λ , we obtain

$$\lambda = \frac{-\beta \pm \sqrt{\beta^2 - 4}}{2}. \tag{27}$$

Now I discuss the parameter β . If it were negative, b would be negative, and hence the torque created by the force would push the pendulum from equilibrium versus pull it towards equilibrium. The later is the required case; therefore, $\beta > 0$. First, let $\beta \geq 2$. In this situation, there is no imaginary part, and the eigenvalues are both negative. The fixed points are hyperbolic, the linearization is justified, and they are categorized as sinks [2]. Second, let $2 > \beta > 0$. We now have eigenvalues that are both real and complex. The fixed points for this β range are no longer hyperbolic, and they are categorized as sink-foci.

Next consider the specific case for fixed points when $(\theta^*, y^*) = ((2n + 1)\pi, 0)$. The Jacobian is

$$\begin{pmatrix} 0 & 1 \\ 1 & -\beta \end{pmatrix}. \tag{28}$$

The characteristic equation is

$$-\lambda(-\beta - \lambda) - 1 = 0. \tag{29}$$

Solving for λ ,

$$\lambda = \frac{-\beta \pm \sqrt{\beta^2 + 4}}{2}. \tag{30}$$

When $\beta > 0$ the eigenvalues are real and of opposite sign. The fixed points when $(\theta^*, y^*) = ((2n + 1)\pi, 0)$ are hyperbolic and categorized as saddles [2].

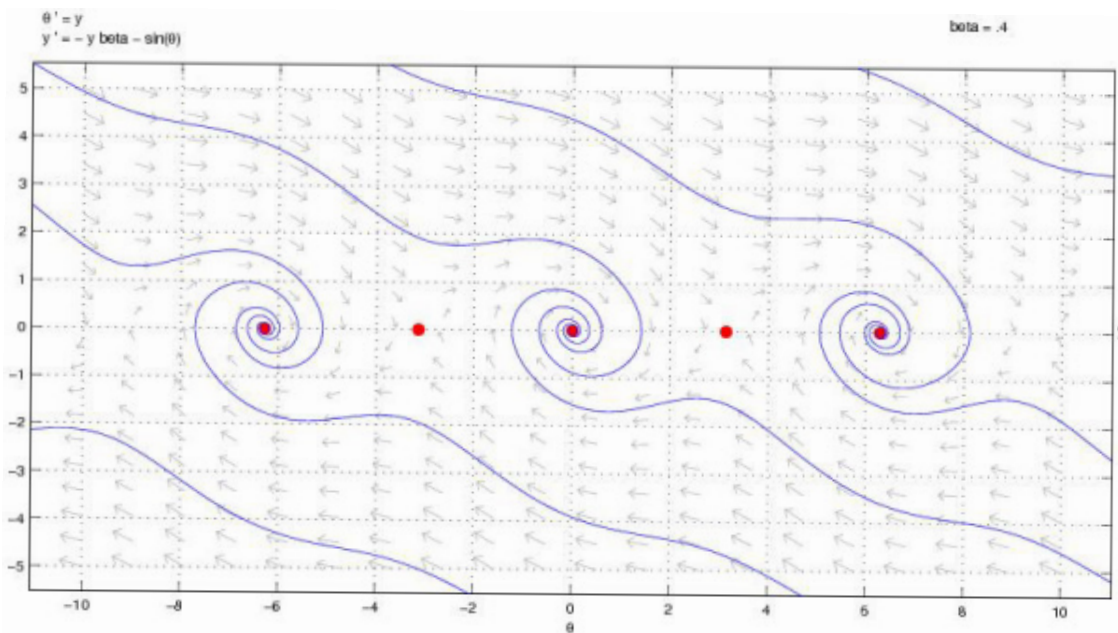


Figure 4: phase plane of damped pendulum with $\beta = .4$

Figure 4 above is the phase plane of eq. (20) with $\beta = .4$. The equilibrium points are saddles at $(\theta^*, y^*) = ((2n + 1)\pi, 0)$ correlating to the analysis. The other equilibrium points at $(\theta^*, y^*) = (2n\pi, 0)$ are sink-foci correlating to analysis. In the top panel of Figure 6 is the linearization about the fixed points of the system of eq. (20) with $\beta = .4$. From left to right in

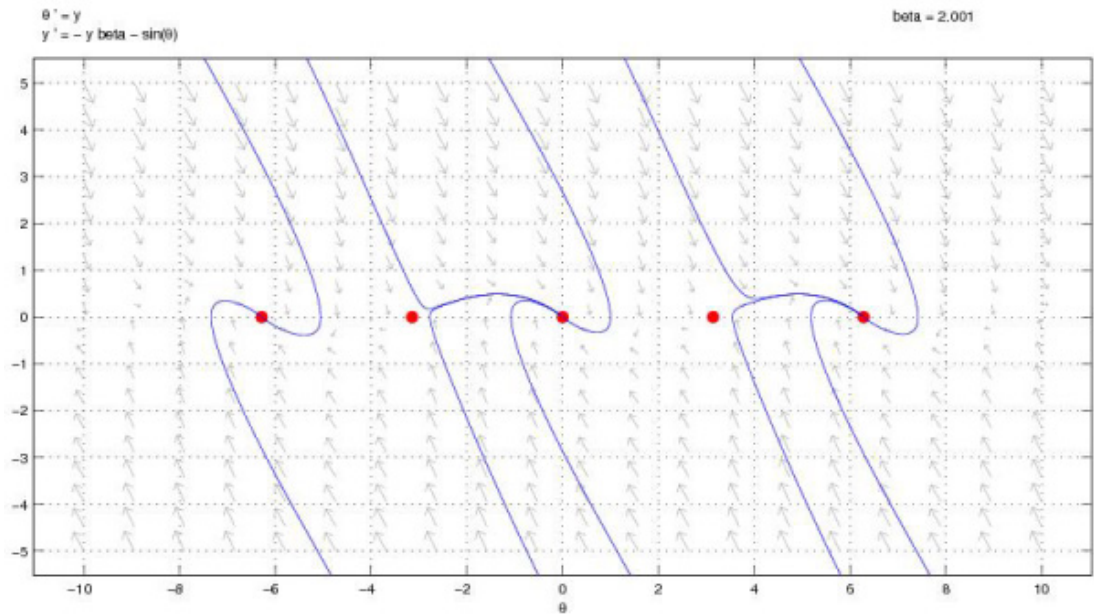


Figure 5: Phase plane of damped pendulum with $\beta = 2.001$

the top panel of Figure 6 is the linearization about the fixed points when $(\theta^*, y^*) = (2n\pi, 0)$ and $(\theta^*, y^*) = ((2n + 1)\pi, 0)$, respectively.

Figure 5 below is the phase plane of eq. (20) with $\beta = 2.001$. The equilibrium points are saddles at $(\theta^*, y^*) = ((2n + 1)\pi, 0)$ correlating to the analysis. The other equilibrium points at $(\theta^*, y^*) = (2n\pi, 0)$ are sinks correlating to analysis. In the bottom panel of Figure 6 is the linearization about the fixed points of the system of eq. (20) with $\beta = 2.001$. From left to right in the bottom panel of Figure 6 is the linearization about the fixed points when $(\theta^*, y^*) = (2n\pi, 0)$ and $(\theta^*, y^*) = ((2n + 1)\pi, 0)$, respectively.

When the Hartman-Grobman theorem reveals nothing about the non-hyperbolic fixed points, compare the Jacobian from the linearization to the phase plane of the system. For the system described by eq. (20) they are the same and the linearization describes the dynamics as well.

Finally answering our initial question, the dynamical system described by eq. (20) is confined to the two dimensional phase plane. By the Poincare-Bendixson theorem, chaos is not possible.

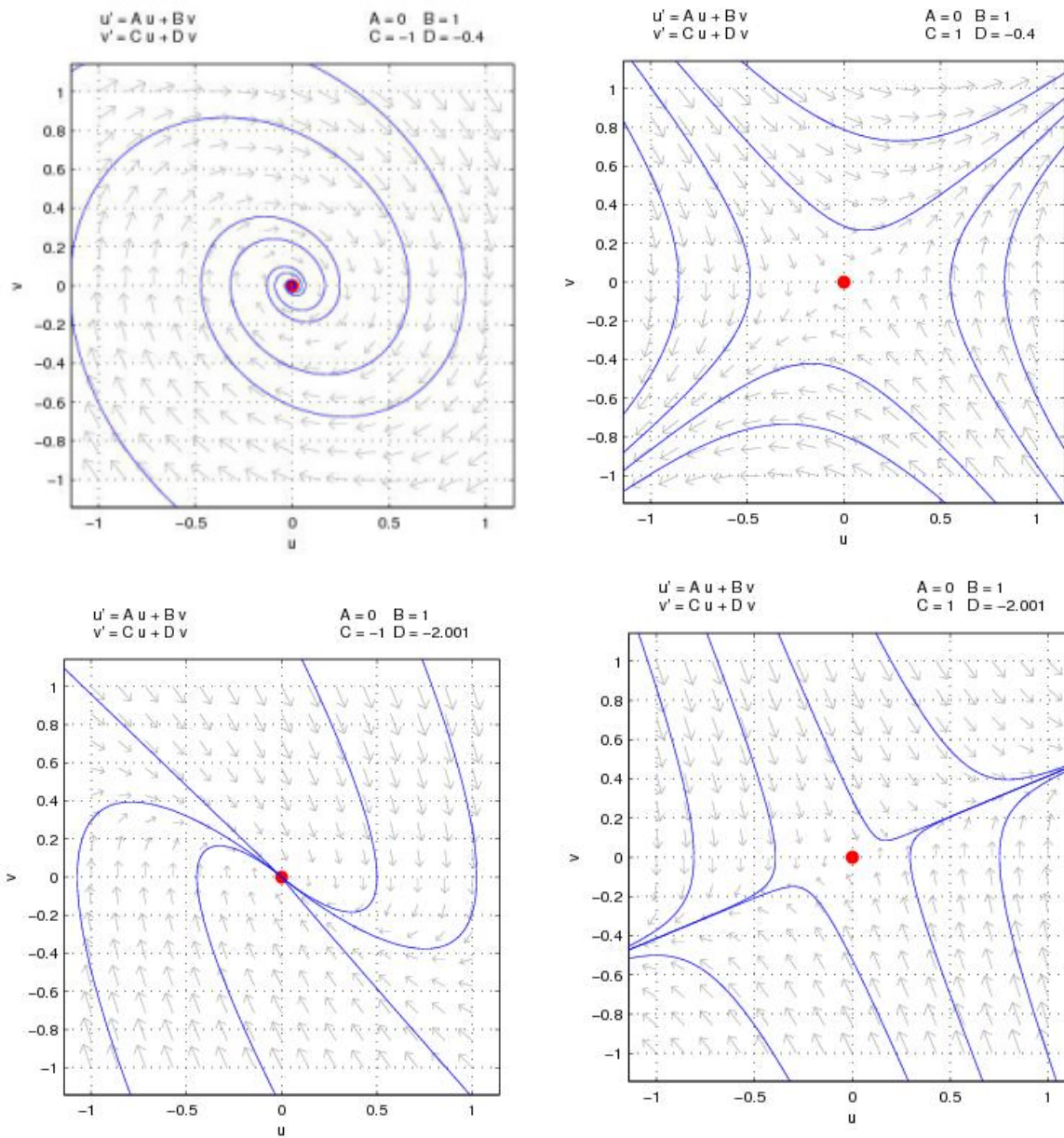


Figure 6: Linearizations about the fixed points *Upper Left* $2n\pi$ when $\beta = .4$, *Upper Right* $(2n + 1)\pi$ when $\beta = .4$, *Bottom Left* $2n\pi$ when $\beta = 2.001$, and *Bottom Right* $(2n + 1)\pi$ when $\beta = 2.001$.

5 The Golden Goose, Chaos

We have finally arrived at the case of the pendulum where there will be no simplifications, $\sin(\theta)$ will not become θ by use of the small-angle approximation, unless the amplitude of the driving force is small. The damping force by will be present as well as the driving force, which until now has been set equal to zero. Let us begin discussing the driving force, $F(t)$. We have already alluded to the fact that the driving force is a function of time, just by use of notation. However, if we allowed the driving force to be constant it would drive the pendulum to some equilibrium position in the case that the amplitude was not great enough to overcome the forces from gravity and damping. If the amplitude were great enough to overcome the opposing forces it would surely drive the pendulum in a repeated motion. Both these scenarios do not include chaos. So we will let the driving force vary with time such that $F(t) = F_0 \cos(\omega * t)$, where F_0 is the amplitude and ω is the driving angular frequency.

Eq. (5) becomes

$$\ddot{\theta} + \frac{b}{m}\dot{\theta} + \frac{g}{r}\sin\theta = \frac{F_0 \cos(\omega * t)}{mr}. \quad (31)$$

Letting $\dot{\theta} = y$, the system described by eq. (31) becomes

$$\dot{\theta} = y, \quad (32)$$

$$\dot{y} = -\frac{b}{m}y - \frac{g}{r}\sin(\theta) + \frac{F_0 \cos(\omega * t)}{mr}. \quad (33)$$

Equations (32) and (33) seem to be a system described by a two dimensional-phase plane as I have written it. The Poincare-Bendixson theorem will not allow chaos in the two-dimensional phase plane. However, note that the system is nonautonomous, and it can be made into a three-dimensional autonomous system by doing the following:

Let $z = \omega * t$. Differentiating with respect to time, $\dot{z} = \omega$. Now the system described by eqs. (32) and (33) becomes

$$\dot{\theta} = y, \quad (34)$$

$$\dot{y} = -\frac{b}{m}y - \frac{g}{r}\sin(\theta) + \frac{F_0 \cos(z)}{mr}, \quad (35)$$

$$\dot{z} = \omega. \quad (36)$$

The Poincare-Bendixson theorem no longer applies since we have a three-dimensional. Chaos is not ruled out, but neither is it guaranteed.

We may now begin the search for chaos. In John Taylor's *Classical Mechanics*, chaos is approached in an extremely elegant way and we follow his approach here, adopting his notation. From eq. (31) let $2\beta = \frac{b}{m}$, $\omega_0^2 = \frac{g}{r}$, and $\gamma\omega_0^2 = \frac{F_0}{mr}$, where $\gamma = \frac{F_0}{mg}$ [3]. Equation (31) becomes

$$\ddot{\theta} + 2\beta\dot{\theta} + \omega_0^2 \sin\theta = \gamma\omega_0^2 \cos(\omega * t). \quad (37)$$

This is a very idealized textbook equation for the motion of a pendulum. We will also discuss a real experimental system known as the EM-50 Chaotic Pendulum constructed by the Daedalon

Corporation. The description of this system can be found in the instruction manual [4]. The differences between the textbook pendulum and the real pendulum take place where the moment of inertia is unknown analytically. The damping constant is just b ; it comes from electromagnetic forces rather than a contact force. Eq. (4) would then be written as

$$I\ddot{\theta} + b\dot{\theta} + mgr \sin \theta = F(t)r, \tag{38}$$

$$\ddot{\theta} + \frac{b}{I}\dot{\theta} + \frac{mgr}{I} \sin \theta = \frac{F_0r}{I} \cos(\omega * t). \tag{39}$$

Adopting again similar notation to Taylor’s *Classical Mechanics*, let $2\beta = \frac{b}{I}$, $\omega_0^2 = \frac{mgr}{I}$, and $\gamma\omega_0^2 = \frac{F_0r}{I}$, where $\gamma = \frac{F_0}{mg}$. We can write eq. (39) in the same form as eq. (37).

Next we begin discussing the parameters we will be using while searching for chaos. Again like Taylor, we let $\omega = 2\pi$. The driving period, $T = \frac{2\pi}{\omega}$, is then equal to one. There is no better choice; this becomes extremely useful for future qualitative analysis. Taylor states that chaos is easy to find when the ω_0 is close to ω . Next we will use a numerical solver to view two solutions to discover that we should let $\omega_0 > \omega$.

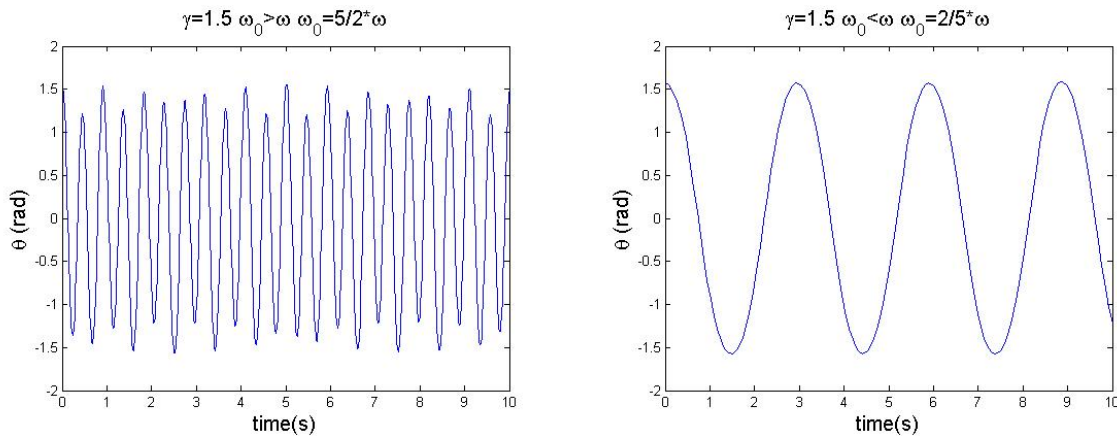


Figure 7: *Left:* Solution with $\omega_0 = \frac{5}{2}\omega$ and *Right:* $\omega_0 = \frac{2}{5}\omega$

In fig. (7) we see that when $\omega_0 > \omega$ the left panel we have a much more erratic behavior that leads to chaos, although chaos is not yet present.

Next we discuss the damping parameter β . It is very evident that we prefer the damping to be less than the natural frequency, ω_0 , of the pendulum, so we are not critically damped or over-damped. It is not necessary though, given the amplitude of the driving force one can select a good damping parameter.

We have chosen $\omega = 2\pi$, and we want $\omega_0 > \omega$, so let $\omega_0 = \frac{4}{3}\omega = \frac{8\pi}{3}$. We want β to be less than the amplitude of the driving force, $\gamma\omega_0^2$, so let $\beta = \frac{\omega_0}{4} = \frac{2\pi}{3}$. When $\gamma = .2$, $\beta < \gamma\omega_0^2$. The parameter that varies in search of a chaotic regime is γ . I have used the above parameters in search of chaos and although I may have found it, the approach through period doubling is unclear and may not exist for the perscribed parameters.

To show a clear approach to chaos, we will adopt the parameters chosen by John R. Taylor in his *Classical Mechanics*. This will also be useful later because Taylor’s parameters were used to set all other parameters from ω_0 in the actual experiment with the EM-50 Chaotic Pendulum.

Taylor’s parameters are defined as $\omega = 2\pi$, $\omega_0 = \frac{3}{2}\omega = 3\pi$, $\beta = \frac{\omega_0}{4} = \frac{3\pi}{4}$ [3], and γ varies. With these parameters, period doubling and chaos are easily seen, the easiest way to see that period

doubling will occur and determine the values when period doubling or chaos occurs is by the use of a bifurcation diagram. Figure (8) was produced using MATLAB and edited files, to model the pendulum system, Programs_14f.m and Programs_14g.m written by Stephen Lynch [5]. From Figure (8) we can see where the bifurcation begins. Figure (9) is a enlarged section of Figure (8), where we can begin determining what values period doubling begins. By inspection of figure (9) it seems below $\gamma = 1.0675$ the period becomes one and above $\gamma = 1.0675$ the period becomes two, meaning that the period has doubled.

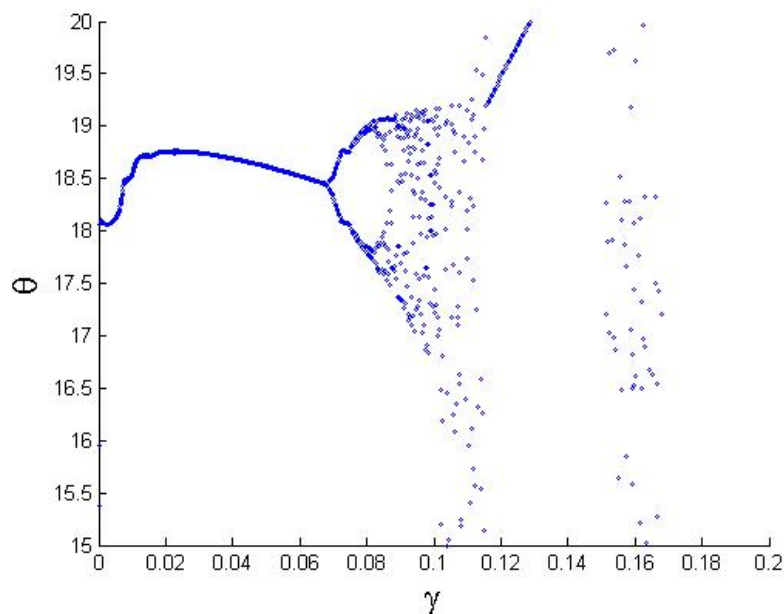


Figure 8: Bifurcation diagram for the damped driven pendulum, note γ has been shifted by one and any value read from the graph should be interpreted as $\gamma_{true} = \gamma_{graph} + 1$

Let us look at some solutions produced using MATLAB's ode45 function. The first is for the parameters stated above, with $\gamma = 1.01$, and $\theta = \dot{\theta} = 0$. In fig. (10), one can see the period is 1 second after the transient part of the solution has decayed. Next look at the solution with the same initial conditions except now $\gamma = 1.07$. Figure (11) shows the solution where, after the transients have decayed, the period is 2 seconds.

We return to fig. (9) again to see where γ will yield a period 4 orbit and it appears to happen when $\gamma > 1.075$. We again plot the solution when $\gamma = 1.07875$ with the same initial conditions as before. In figure (12), the solution has been scaled for the time interval shown, and one can approximately tell the period is 4 seconds.

Another method to determine the period is by the use of the phase plane $(\theta, \dot{\theta}) = (\theta, \omega)$. Figure (13) shows the phase plane for the first solution with $\gamma = 1.01$. Looking at the darkest line shows the orbit, with period 1, after the transient has decayed. Fig. (14) shows the orbit for $\gamma = 1.07$. The zoomed right panel shows that there are two points which the pendulum is passing through on its period-2 orbit.

We could continue to period 8 and period 16, but the numerical solutions are becoming less accurate. This period-doubling that occurs when increasing γ is what many authors, including Taylor, call the road to chaos. Before we continue in search of chaos we can make a Poincare

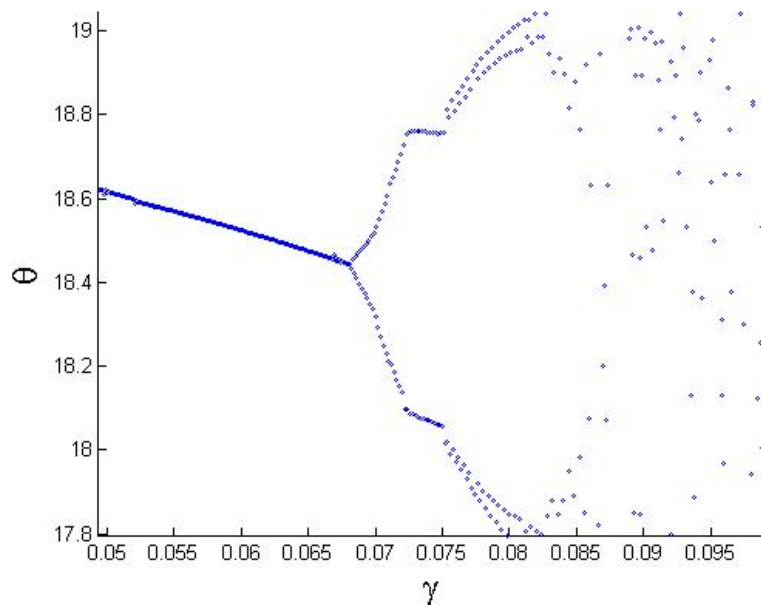


Figure 9: Bifurcation diagram for the damped driven pendulum, note γ has been shifted by one and any value read from the graph should be interpreted as $\gamma_{true} = \gamma_{graph} + 1$

section by numerical methods. A Poincare section is made by following the variable of interest such as θ and θ in our case at intervals of time instead of as continuous time [3]. For example, if we choose the time interval to be the period of a function of $\sin(2\pi * t)$, we know $\sin(2n\pi)$ is always equal to zero, where $n = \text{integers}$, beginning at one. The Poincare section for this example has a single stable fixed point, correlating to the period of the motion. Thus the number of fixed points in a Poincare section will tell us information about the period of the motion. The following figures are produced using edited code, Programs_14d.m written by Stephen Lynch [5]. Figure (15) is the Poincare section with $\gamma = 1.01$, one can see as the transient decays, the iterates of the Poincare section approach a fixed point, this tells us the period is one. Figure (16) is the Poincare section with $\gamma = 1.07$, we zoom in to see the section approaching two fixed points, this tells the period is two, as we have verified before.

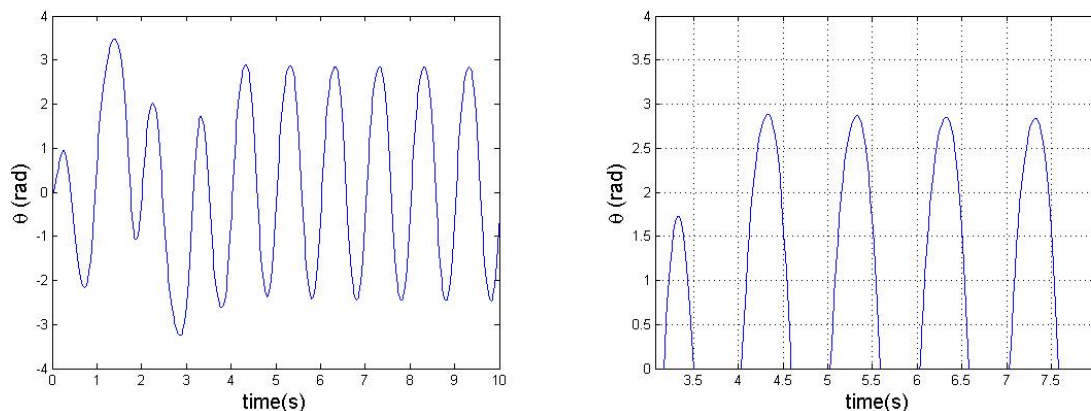


Figure 10: *Left:* Solution with $\gamma = 1.01$, and $\theta = \dot{\theta} = 0$ and *Right:* zoom of the solution to see period of 1 second.

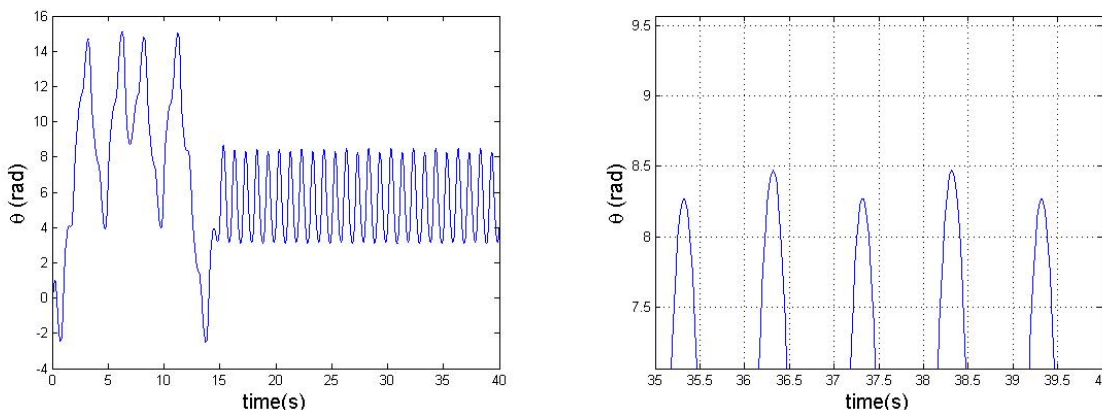


Figure 11: *Left:* Solution with $\gamma = 1.07$, and $\theta = \dot{\theta} = 0$ and *Right:* zoom of the solution to see period of 2 second.

So far we have discussed how to obtain the solution, the phase plane, and the Poincare section. Let us go on a search for chaos armed with all of these tools. First, return to fig. (9) and choose from the bifurcation diagram $\gamma = 1.16$. As before we shall plot the solution, phase plane, and Poincare Section for this specific γ as well as $\theta = \dot{\theta} = 0$ for initial conditions. Figure (17) is the solution. Figure (18) is the phase plane. Figure (19) is the Poincare section. In fig. (17) the motion does not look predictable, in fig. (18) phase plane is full, and in fig. (19) the Poincare section is also full. This definitely seems to be a chaotic solution to the pedulum equations. But, how can one prove that we have a chaotic solution? Aleksandr Lyapunov defined an exponent in which the difference between two solutions behaves exponentially.

$$\Delta\theta(t) \approx Ce^{\lambda*t} \tag{40}$$

Where λ is the Lyapunov exponent [2]. There are three defining behaviors of systems depending on the Lyapunov exponent. If $\lambda < 0$ the solution is attracted to a fixed point or a periodic orbit. Note that $e^{\lambda*t} \rightarrow 0$ as $t \rightarrow \infty$, for negative λ , so $\Delta\theta(t) \rightarrow 0$, and the solutions becomes identical. If $\lambda = 0$ the solution is attracted to a fixed point, $e^0 = 1$ and $\Delta\theta(t)$ is a constant. The difference

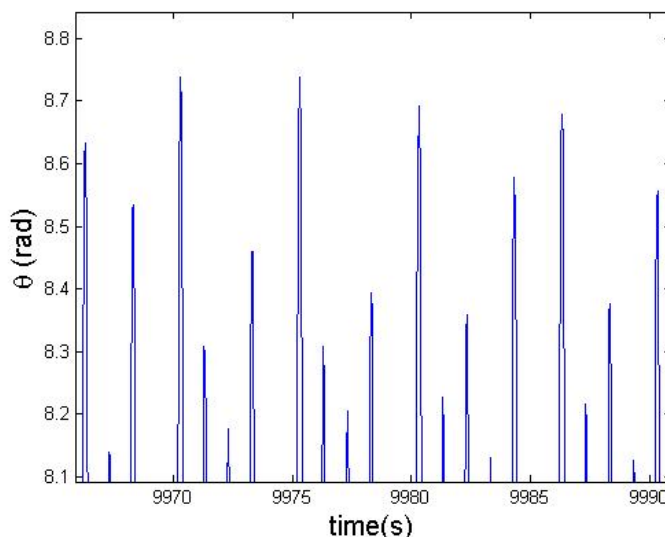


Figure 12: Solution with $\gamma = 1.07875$, and $\theta = \dot{\theta} = 0$.

between the solutions remains constant. Finally, if $\lambda > 0$ the solution is chaotic, $e^{\lambda t} \rightarrow \infty$ as $t \rightarrow \infty$ for positive λ . The difference between solution increases exponentially for some time, eventually saturation of the separation occurs.

One could produce solutions from MATLAB code with slightly different initial conditions and proceed to find the Lyapunov coefficient; however, it is much more interesting to do so for a real system. From here we will continue to determine the Lyapunov coefficient of two solutions, but it will be done for that of two solutions that come from actual data from the EM-50 Chaotic Pendulum, eq. (37), which is modelled identically to the theoretical pendulum, eq. (39).

Figure (29) is of the EM-50 Chaotic Pendulum. M is a mass connected to a rod. C is a magnet which is driven by drive coils, E , which is the source of the driving force. B is a non-rotating copper plate. Its distance relative to the magnet is controlled by F . When the magnet rotates and the copper plate remains stationary eddy current is lost. B and its position are the source of damping. A and D combine to collect data in the form of the position and velocity of disk A , this correlates to measurements of M .

Figures (20) and (21) are the time versus measured angles, θ , for two solutions of the EM-50 Chaotic Pendulum. The initial conditions are $\theta = \dot{\theta} = 0$. Where the difference between the initial conditions is less than $\pm .00001$ radians. Actually the pendulum is allowed to settle into its resting downward position which should be two identical initial conditions but the system that collects the measurements of θ has accuracy on the order of .0001 radians. The data collected correlates this fact; however, we do not assume that we know the measurement of θ any more accurately than to .0001 radians. As stated above, we know the difference between the initial conditions is less than $\pm .00001$ radians. We denote solution one as the red curve in fig. (20) as θ_1 and solution two as the blue curve in fig. (21) as θ_2 . Figures (22) through (24) are solutions one and two plotted together at different time intervals to show the divergence and the similarities of the solutions. Let $\Delta\theta(t)$ denote the absolute value of the difference between the solutions, $\Delta\theta(t) = |\theta_1 - \theta_2|$. Figure (25) is a plot of the difference between the solutions. Does fig. (25) actually fit the model of an exponential to a positive power? We can do some math from eq. (40) and simplify this question.

Take the natural log of both side of eq. (40):

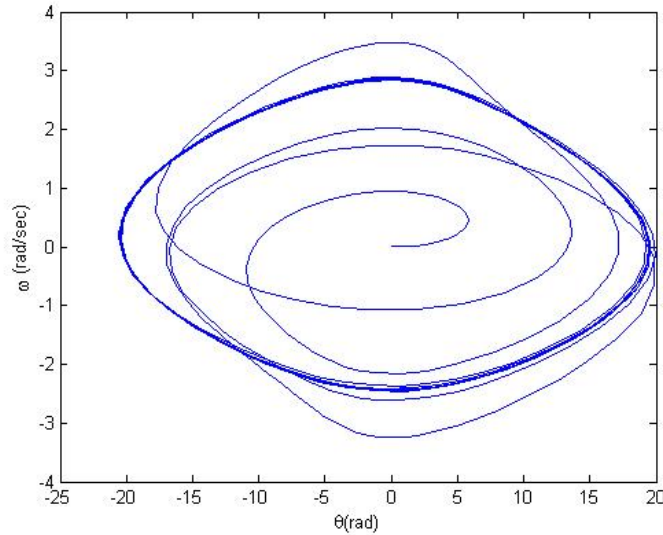


Figure 13: Phase plane with $\gamma = 1.01$, and $\theta = \dot{\theta} = 0$.

$$\ln(\Delta\theta(t)) = C\lambda * t \quad (41)$$

Now we can ask if there is an increasing linear region if we plot the $\ln(\Delta\theta(t))$. Figures (26) and (27) are the plots of the natural log of the difference between the solution at different time intervals. In the zoomed time interval fig. (27) one can see a linear region for approximately the first 2000 data points measured. We fit a linear curve, colored blue, to a suspected linear region and plot it in fig. (28). The slope is positive; therefore, $C\lambda$ is positive. λ is also positive. The existence of a positive Lyapunov coefficient proves the pendulum system was in a chaotic regime.

6 Conclusion

A completely deterministic system can have chaotic dynamics as well as extremely well understood linear dynamics. Everything that was expected in the simplified and non-linear regime of pendulum was discovered and proved. Chaos was discovered in theory and experimentally.

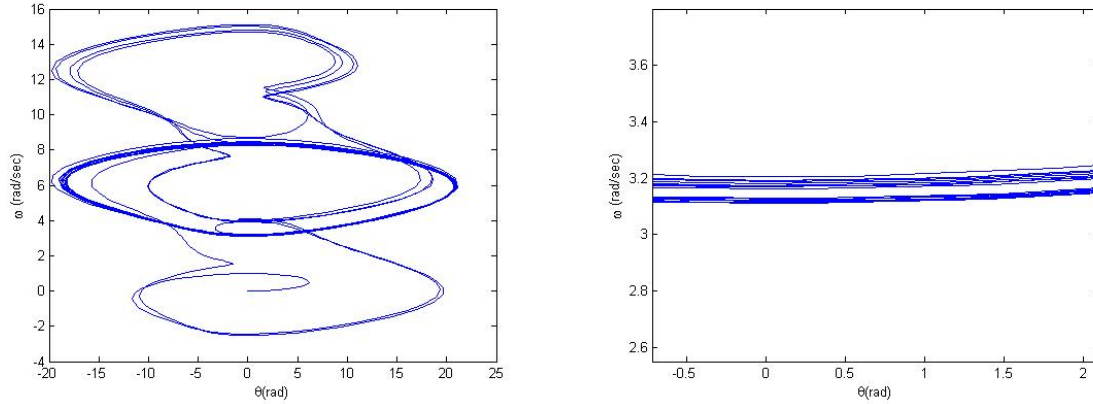


Figure 14: *Left*: Phase plane with $\gamma = 1.07$, and $\theta = \dot{\theta} = 0$ and *Right*: zoom of the phase plane to see period of 2 second.

References

- [1] Strogatz, Steven. *Nonlinear Dynamics and Chaos*. Westview Pr, 2000. p. 160. Print.
- [2] Meiss, James. *Differential Dynamical Systems*. 1st. Philedelphia, PA: SIAM, 2007. p. 114,220. Print.
- [3] Taylor, John. *Classical Mechanics*. 2nd. Univ Science Books, 2005. p. 464,495. Print.
- [4] Blackburn, James, and H Smith. *Instruction Manual for EM-50 Chaotic Pendulum*. Salem, MA: Daedalon Corporation, 1998. Print.
- [5] Lynch, Stephen. *Dynamical Sytems with Applications Using Matlab*. New York, NY: Birkhauser Boston, 2004. p. 317-319. Print.

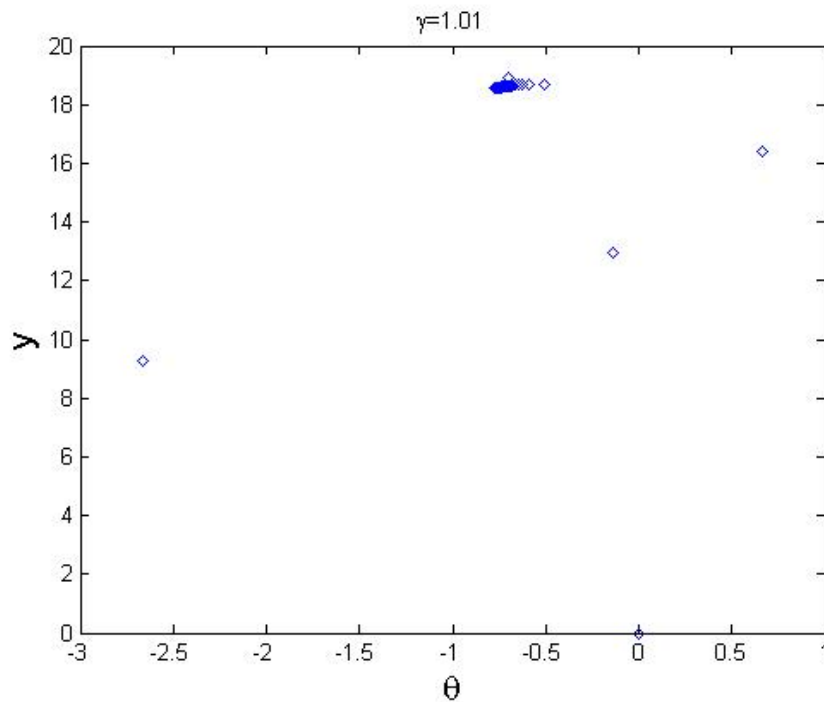


Figure 15: Poincaré section with $\gamma = 1.01$, and $\theta = \dot{\theta} = 0$.

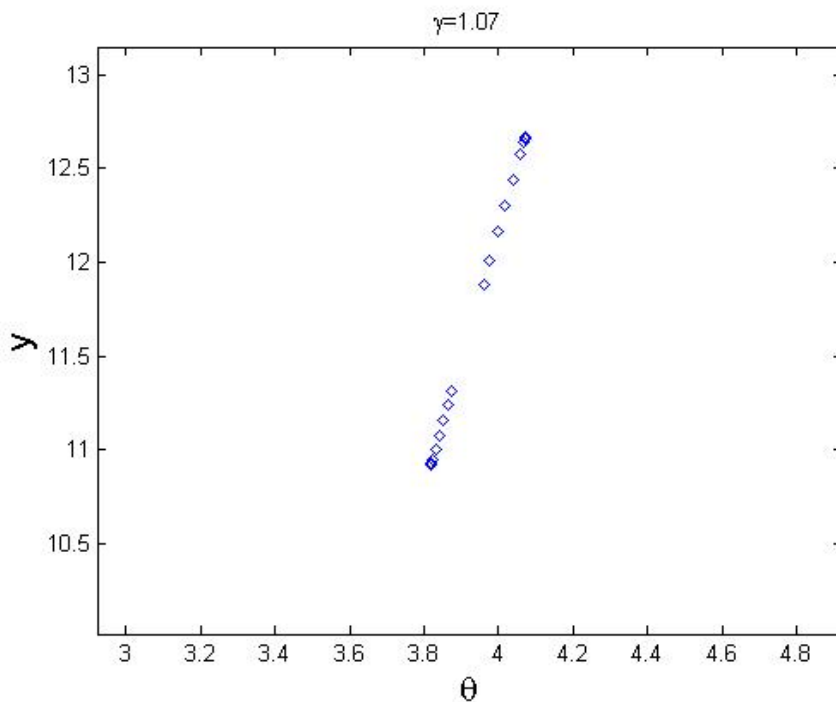


Figure 16: Poincaré section with $\gamma = 1.07$, and $\theta = \dot{\theta} = 0$.

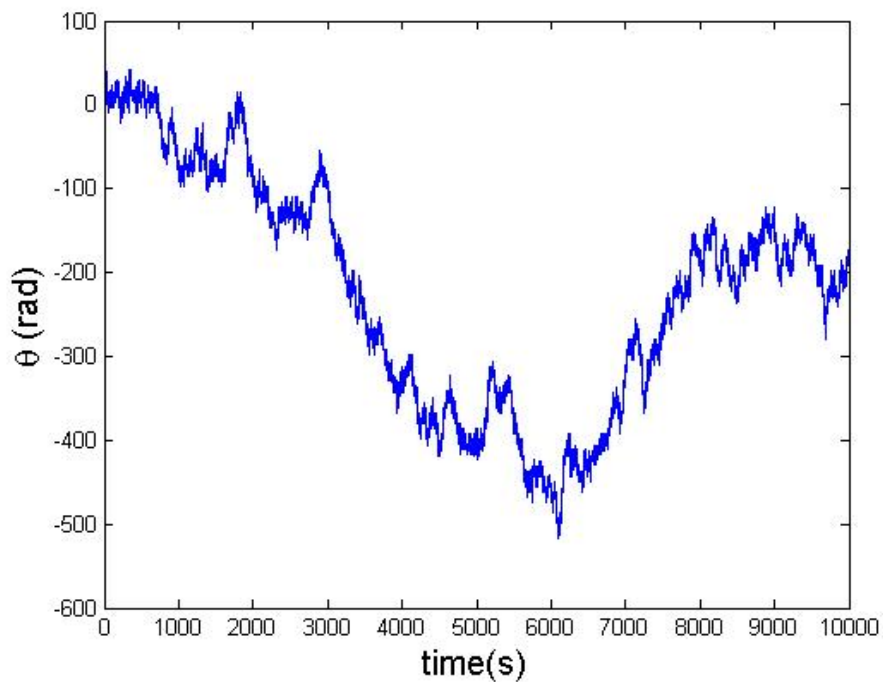


Figure 17: Solution with $\gamma = 1.16$, and $\theta = \dot{\theta} = 0$.

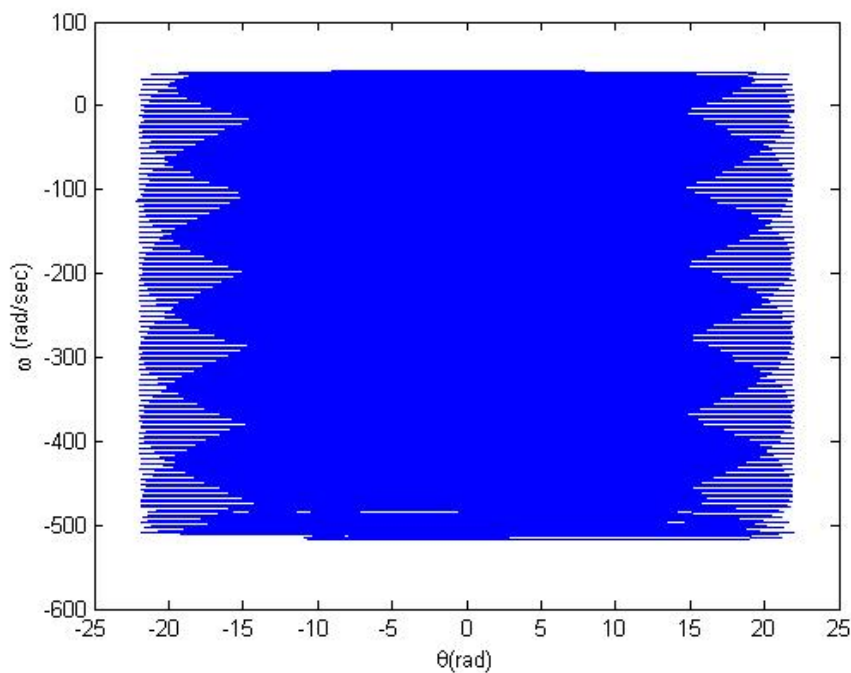


Figure 18: Phase plane with $\gamma = 1.16$, and $\theta = \dot{\theta} = 0$.

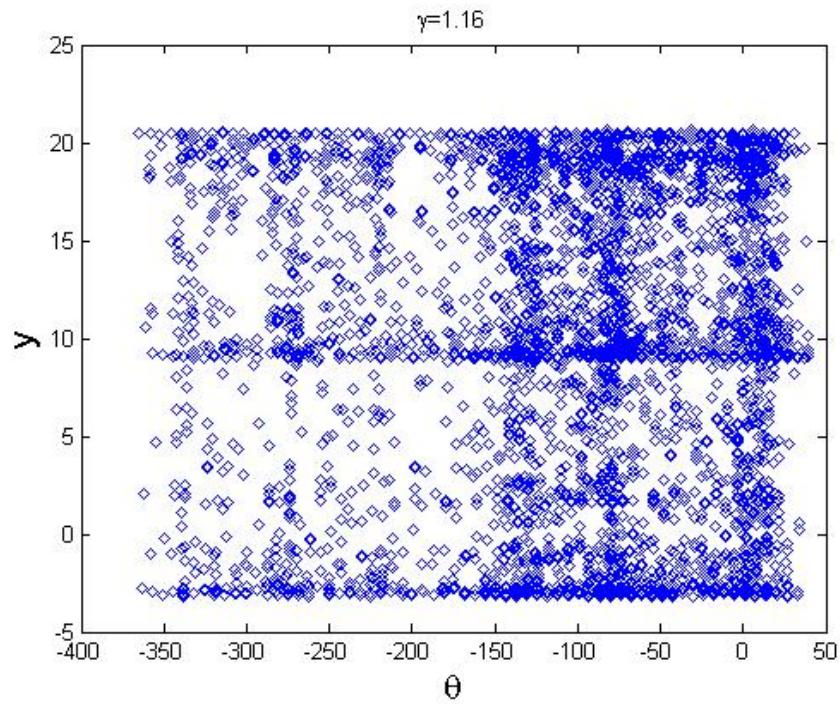


Figure 19: Poincaré section with $\gamma = 1.16$, and $\theta = \dot{\theta} = 0$.

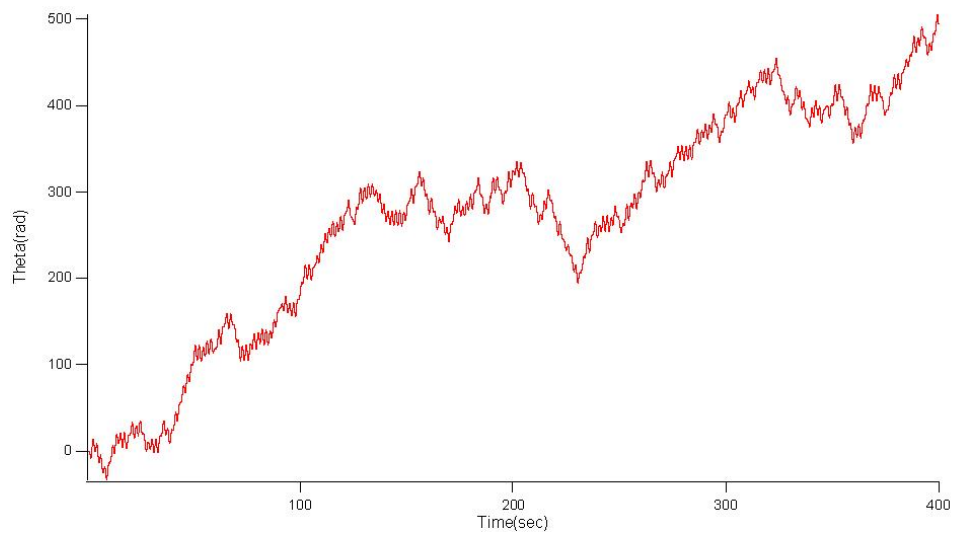


Figure 20: Solution one of the EM-50 Chaotic Pendulum.

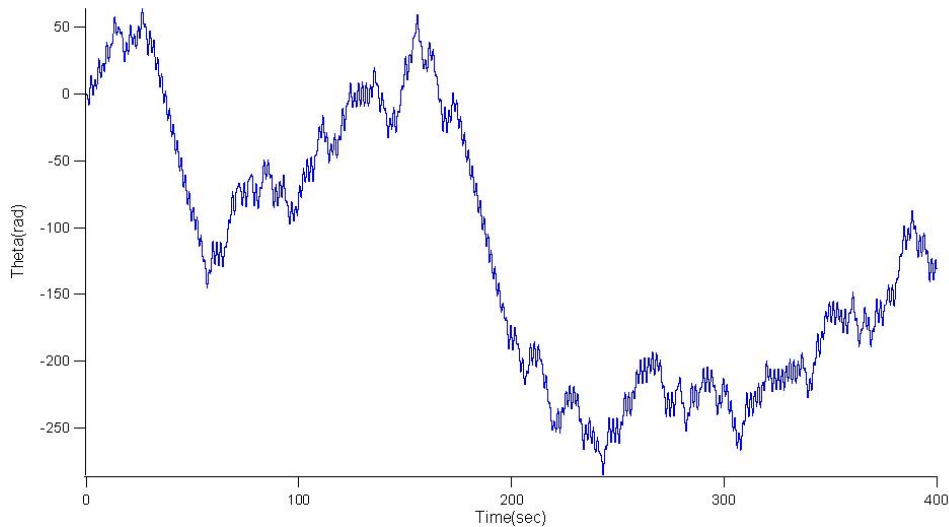


Figure 21: Solution two of the EM-50 Chaotic Pendulum.

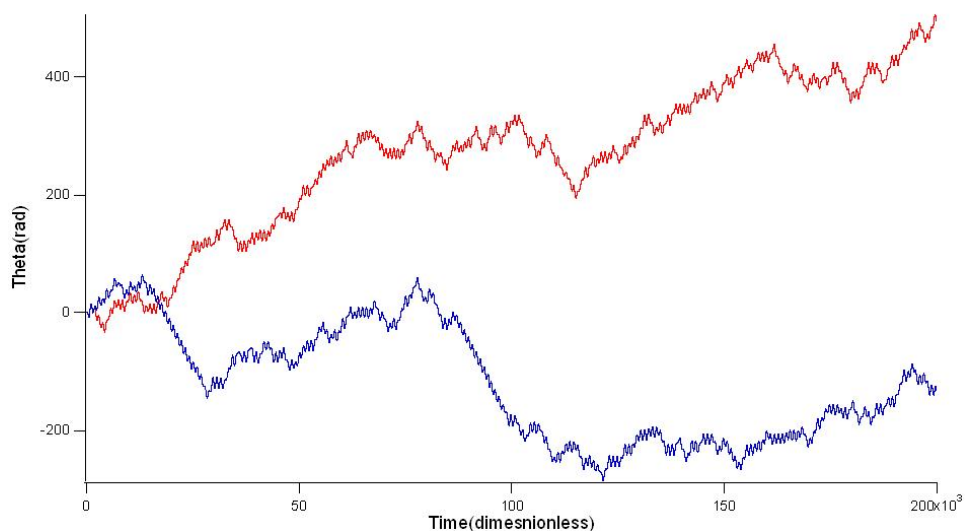


Figure 22: Both solutions of the EM-50 Chaotic Pendulum.

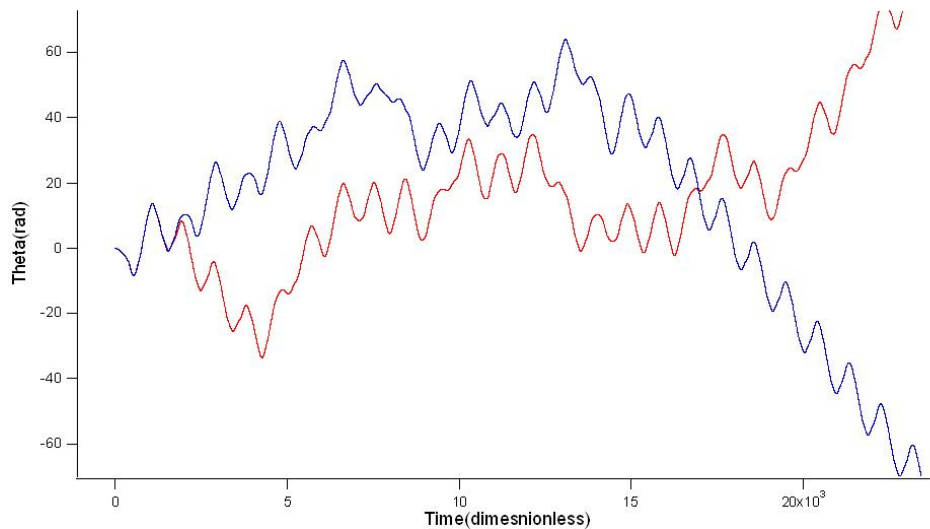


Figure 23: Both solutions of the EM-50 Chaotic Pendulum.

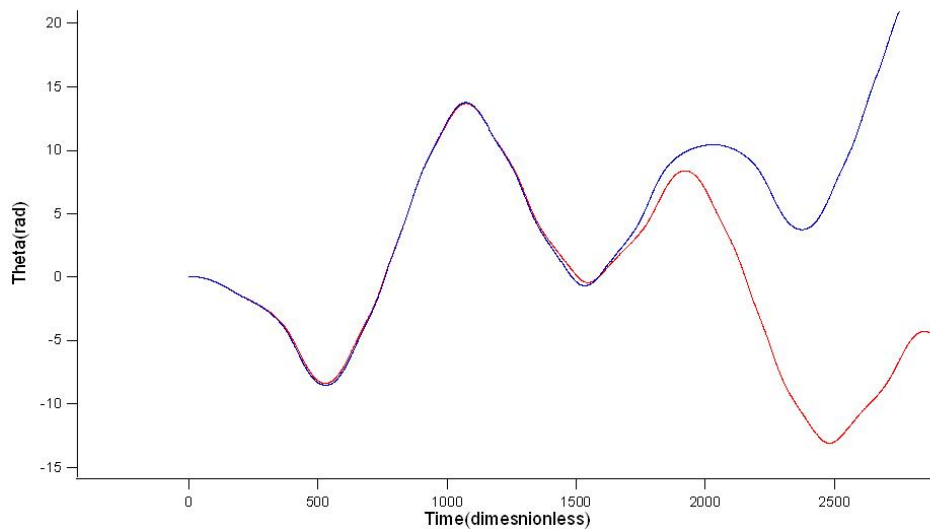


Figure 24: Both solutions of the EM-50 Chaotic Pendulum.

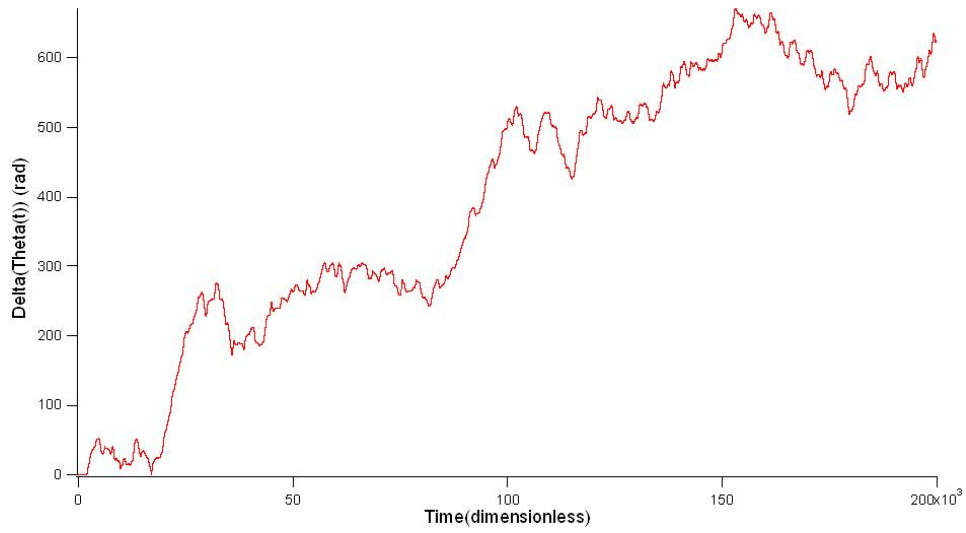


Figure 25: Difference of the two solutions.

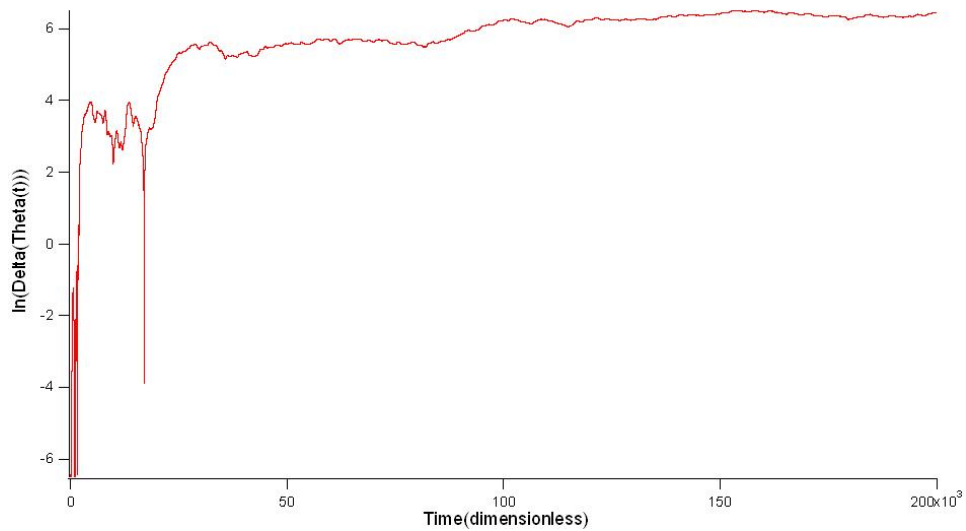


Figure 26: The natural log of the difference of the two solutions.

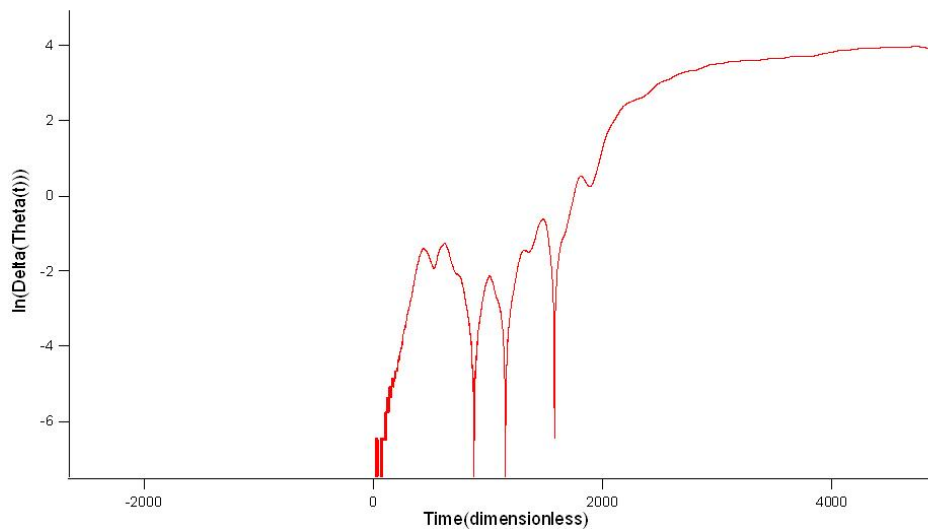


Figure 27: The natural log of the difference of the two solutions.

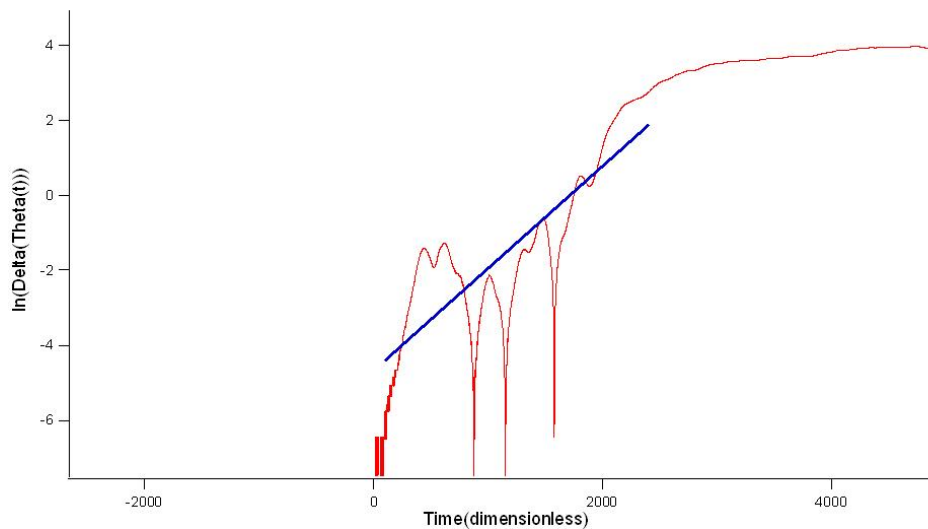


Figure 28: The natural log of the difference of the two solutions with a fitted curve for a suspected linear region.

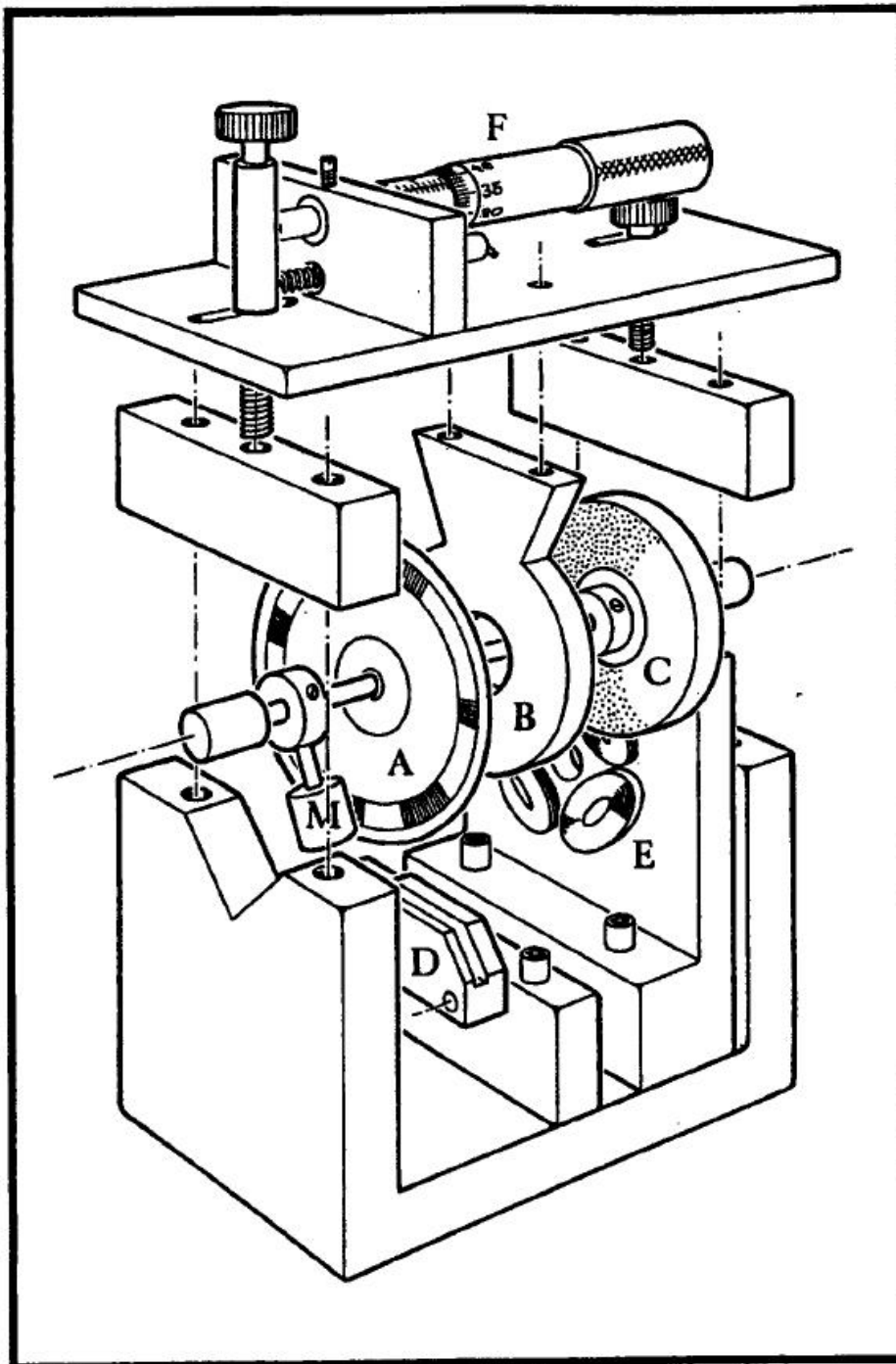


Figure 29: Schematic of the EM-50 Chaotic Pendulum